The thermal mode crucial influence on the ZnSeS QDs formation

Maksym Chylii
Center of Materials and Nanotechnologies, Faculty of Chemical Technology
University of Pardubice
Pardubice, Czech Republic
Maksym.Chylii@upce.cz

Liudmila Loghina
Center of Materials and Nanotechnologies, Faculty of Chemical Technology
University of Pardubice
Pardubice, Czech Republic
Liudmila.Loghina@upce.cz

Anastasia Kaderavkova
Center of Materials and Nanotechnologies, Faculty of Chemical Technology
University of Pardubice
Pardubice, Czech Republic
Anastasia.Kaderavkova@upce.cz

Jakub Houdek
Center of Materials and Nanotechnologies, Faculty of Chemical Technology
University of Pardubice
Pardubice, Czech Republic
st34492@student.upce.cz

Miroslav Vlcek
Center of Materials and Nanotechnologies, Faculty of Chemical Technology
University of Pardubice
Pardubice, Czech Republic
Miroslav.Vlcek@upce.cz

***Abstract*—The qualitative and quantitative diversity of existing methods for the synthesis of chalcogenide nanomaterials is constantly being updated. Attempts to improve an already functioning synthesis scheme may lead to the emergence of a new promising directions. It turned out that the ability of substituted thio- and selenoureas to form stable complexes with metal carboxylates can allow one-pot and hot-injection methods to be combined in the ZnSeS quantum dots (QDs) synthesis. After the formation of zinc linoleate complexes with various substituted thio- and selenoureas in a single reaction system at relatively low temperatures (80 °C), we introduced them into a medium heated to the desired temperature. The complexes decomposing at different rates led to the formation of ZnSeS QDs of various shapes and sizes. Despite these differences, the nanocrystals grew in the same cubic phase at different nucleation and growth temperatures. It was demonstrated that even $ZnSe_{0.1}S_{0.9}$ and $ZnSe_{0.3}S_{0.7}$ QDs prepared at such low, for the growth of chalcogenide semiconductors, temperatures (160 °C and 180 °C) have a narrow size distribution and a good quantum yield (PL QY up to 24 %). In general, the optical characteristics of the synthesized nanomaterials enable further development of this synthesis method and transfer of it to other compositions.**

Keywords— ZnSeS quantum dots, methodology, substituted thioureas, substituted selenoureas, photoluminescence

I. Introduction

The progress of science is always determined by the level of demand for the properties of materials, each of which is preceded by multivektor fundamental research. Nowadays, chalcogenide quantum dots (QDs) can be synthesized by an impressive number of methods, determining their structure and properties in advance, thereby ensuring their application in the creation of biological labels [1], LEDs [2, 3], displays [4], solar cells [5], photodetectors [6], proton, gamma, or neutron scintillators [7 - 9], *etc*.

The synthesis of QDs in an organic medium provides many opportunities for creating binary and multi-component compositions. The nature of the solvent determines the coordination of molecules or does not affect it at all [10]. The reactivity of the reagents makes it possible to control the growth kinetics of QDs [11] and, consequently, determines their size and the gradient of the atoms' distribution in the nanocrystal. Additional multitasking components, acting in parallel as both a solvent and as a building material for the formation of a protective ligand shell, can also be used in various combinations. The size, shape, and, as a result, properties can also be determined by the method of supplying the initial components to the growth medium. The advantages of the one-pot method are clear: all components are in the growth medium and allow the control of the medium saturation with molecules of the initial components. Introducing one or more components into a heated medium (hot-injection method) provides instant nucleation and stable growth of a nanocrystal in the shortest time intervals [12]. However, combining these separate methods can lead to unexpected results.

In this study, we combine these two methods by a "transit stop" - the possibility to create an intermediate complex that precedes the introduction of molecular zinc sulfides and selenides into the nucleation and nanocrystal growth medium. Combining various substituted thio- and selenoureas in a complex with zinc linoleate in a wide temperature range (160 - 280 °C), $ZnSe_{0.1}S_{0.9}$ and $ZnSe_{0.3}S_{0.7}$ QDs differing in shape and size have been prepared. The blue shift of the photoluminescence (PL) signals indicates different decomposition rates of the complexes, thereby providing an uneven anion distribution gradient (heterogeneous alloys) and increasing the percentage of zinc sulfide in the direction from the core to the surface of the nanocrystal.

II. Experiment

A. Chemicals

Selenium (Se, 99.9 %), phenyl isothiocyanate (PhNCS, 98 %), morpholine (99 %), benzylamine (99 %), allyl isothiocyanate (99 %), zinc oxide (ZnO, 99 %), 1-octadecene (ODE, technical grade, 90 %), linoleic acid (LA, technical grade 60-74 %), oleylamine (OAm, technical grade, 90 %), Solvents were purchased from Fisher Scientific and used without further purification. (*Z*)-N-(octadec-9-en-1-yl)morpholine-4-carboselenoamide (*SU1*), 1-allyl-3-butylthiourea (*TU1*), (Z)-1-benzyl-3-(octadec-9-en-1-

yl)selenourea (*SU2*) and N-phenylmorpholine-4-carbothioamide (*TU2*) were synthesized in our laboratory according to previously published methods [13]. Syntheses of QDs were carried out using standard Schlenk techniques under an argon atmosphere.

B. *Synthesis of $ZnSe_{0.1}S_{0.9}$ QDs*

Zinc oxide (ZnO, 7.34 g, 0.09 mol), linoleic acid (LA, 101 g, 0.36 mol) and 180 ml ODE were placed in a reaction flask (500 ml). The mixture was degassed for 1 hour at room temperature with intense stirring, then for 1 hour at 150 °C to remove the water released during the formation of linoleate. A homogeneous 0.3 M solution of zinc linoleate was further stored under an argon atmosphere and it was periodically taken as a zinc precursor.

Schlenk flask (50 ml) was loaded with 15 ml of 0.3M solution of zinc linoleate (0.0045 mol), (*Z*)-N-(octadec-9-en-1-yl)morpholine-4-carboselenoamide (*SU1*, 0.13 g, 0.0003 mol), previously dissolved in a mixture of 0.5 ml OAm and 1 ml ODE, and 1-allyl-3-butylthiourea (*TU1*, 0.47 g, 0.0027 mol), previously dissolved in the solution of 0.5 ml OAm and 1 ml ODE. The reaction mixture was degassed for 10 min at room temperature, then it was heated to 80 °C and stirred for 30 min in an Ar atmosphere. Further, the reaction mixture was placed in the Wood's metal bath preheated to the selected temperature and stirred for 30 minutes. Throughout the whole process, samples were taken to monitor the progress of nucleation and growth. Then the mixture was allowed to cool and transferred to an equal volume of $CHCl_3$, and finally, QDs were precipitated with acetone. Next, precipitates separated by centrifugation were dissolved in a minimum amount of $CHCl_3$ and precipitated again with acetone. This purification process was repeated two more times to remove solvent and by-products. Finally, purified QDs were dried in a vacuum for 2 hours. The mass of $ZnSe_{0.1}S_{0.9}$ QDs was 0.71 – 0.93 g. The excess in the mass of the product was due to the protective ligand (zinc linoleate) shell.

C. *Synthesis of $ZnSe_{0.3}S_{0.7}$ QDs*

The preparation method of $ZnSe_{0.3}S_{0.7}$ QDs was similar to that described above with the following ratios of components: 15 ml of 0.3M solution of zinc linoleate (0.0045 mol), (*Z*)-1-benzyl-3-(octadec-9-en-1-yl)selenourea (*SU2*, 0.42 g, 0.0009 mol in a mixture of 1 ml OAm and 0.5 ml ODE) and *N*-phenylmorpholine-4-carbothioamide (*TU2*, 0.47, 0.0021 mol in a mixture of 1 ml OAm and 0.5 ml ODE). The mass of $ZnSe_{0.3}S_{0.7}$ QDs was 0.78 – 1.02 g.

III. RESULTS AND DISCUSSIONS

A. *Synthesis and crystalline structure of $ZnSe_{0.1}S_{0.9}$ and $ZnSe_{0.3}S_{0.7}$ QDs*

The structure of substituted thio- and selenoureas plays a key role in this method of ZnSeS QDs synthesis. Thiourea and selenourea functional group -C=S(Se) forms stable in time bidentate complexes, allowing the control of the process of their decomposition into molecular sulfides and selenides at a given temperature. Although this study is only at the beginning, it can already be stated that the crucial role in the kinetics of the decomposition of such complexes is assigned to the structure of substituents. Using thio- and selenoureas with different substituent structures, we observed an ambiguous formation of ZnSeS QDs (Fig. 1).

It was found that when a pair of thio-selenoureas is retained, the temperature affects non-linearly the decomposition of the complexes. For example, with an increase in the $ZnSe_{0.1}S_{0.9}$ QDs synthesis temperature from 160 °C to 220 °C, the average size of QDs noticeably increases from 2.52 nm to 4.04 nm, then the growth slows down, and the size of QDs reaches 4.15 nm at 280 °C. At the same time, the crystal structure (Fig. 2a), as well as the pyramidal shape (Fig. 2b-i) of the nanocrystal, remain unchanged.

X-Ray diffraction patterns (XRD) were registered using PANalytical EMPYREAN powder X-Ray diffractometer (ALMELO, Netherlands) with Cu-Kα radiation (λ = 1.5418

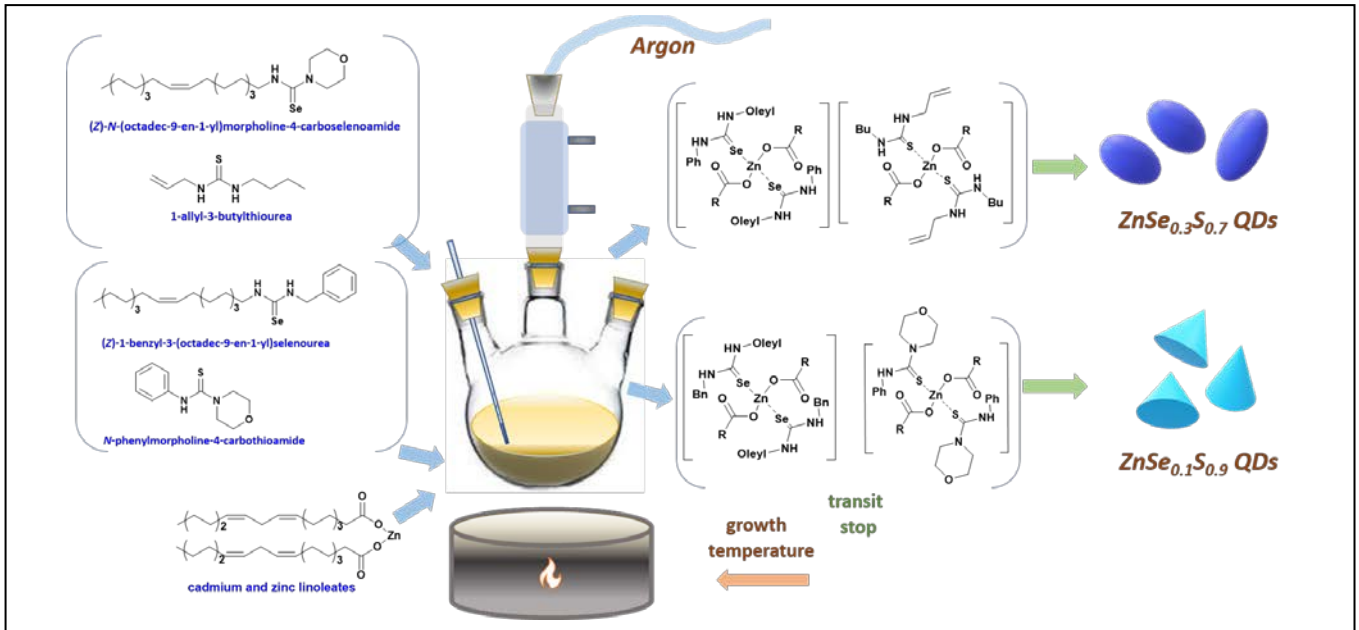

Fig. 1. The schematic illustration of ZnSeS QDs synthesis.

Å). The $ZnSe_{0.1}S_{0.9}$ and $ZnSe_{0.3}S_{0.7}$ nanopowders (Fig. 2a and

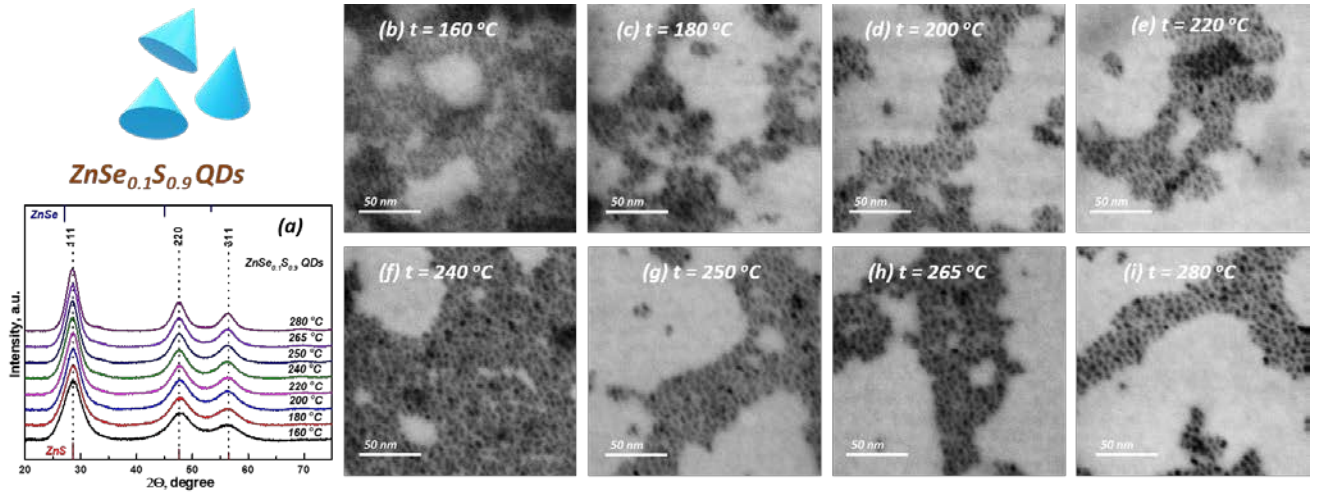

Fig. 2. XRD patterns of $ZnSe_{0.1}S_{0.9}$ QDs (a); STEM images of $ZnSe_{0.1}S_{0.9}$ QDs prepared at 160 °C (b), 180 °C (c), 200 °C (d), 220 °C (e), 240 °C (f), 250 °C (g), 265 °C (h), 280 °C (i).

Fig. 3a) possess a face-centered cubic structure like bulk ZnS (ICSD: 108733) and ZnSe (ICSD: 188389) with a space group F43*m*. As can be seen from Figure 2a, the XRD spectrum for $ZnSe_{0.1}S_{0.9}$ QDs consists of 3 broad peaks at 2θ values of 28.6º, 47.6º and 56.3º which are respectively attributed to (111), (022) and (113) crystallographic planes. Their position is almost identical to the position of the diffraction peaks of these planes in ZnS (ICSD: 108733). With a rise in the growth temperature of $ZnSe_{0.3}S_{0.7}$ QDs up to 220 °C, a significant increase in the average size from 2.87 to 3.73 nm was observed (Table 1). Above 220 °C, the average size of QDs slightly decreases. Obviously, the supply of molecular sulfides and selenides into the growth medium occurs unequable at relatively low temperatures and stabilizes at growth temperatures above 220 °C. The position of the diffraction peaks of the $ZnSe_{0.3}S_{0.7}$ QDs (Figure 3a) shifts towards smaller angles (28.3º, 47.2º and 55.8º) and brings them closer to the position of the diffraction peaks of ZnSe (ICSD: 108733) [13]. No other diffraction peaks were detected in the XRD patterns, which gives evidence of the successful formation of impurity-free Zn-Se-S alloyed QDs.

The chemical compositions of the $ZnSe_{0.1}S_{0.9}$ and $ZnSe_{0.3}S_{0.7}$ nanopowders were determined by X-Ray photoelectron spectroscopy (XPS, ESCA 2SR, Scienta-Omicron, Sweden) by monochromatic Al Kα source (1486.6 eV). The QDs were pressed into C tape for the XPS measurements. The binding energy scale was referenced to adventitious carbon (284.8 eV).

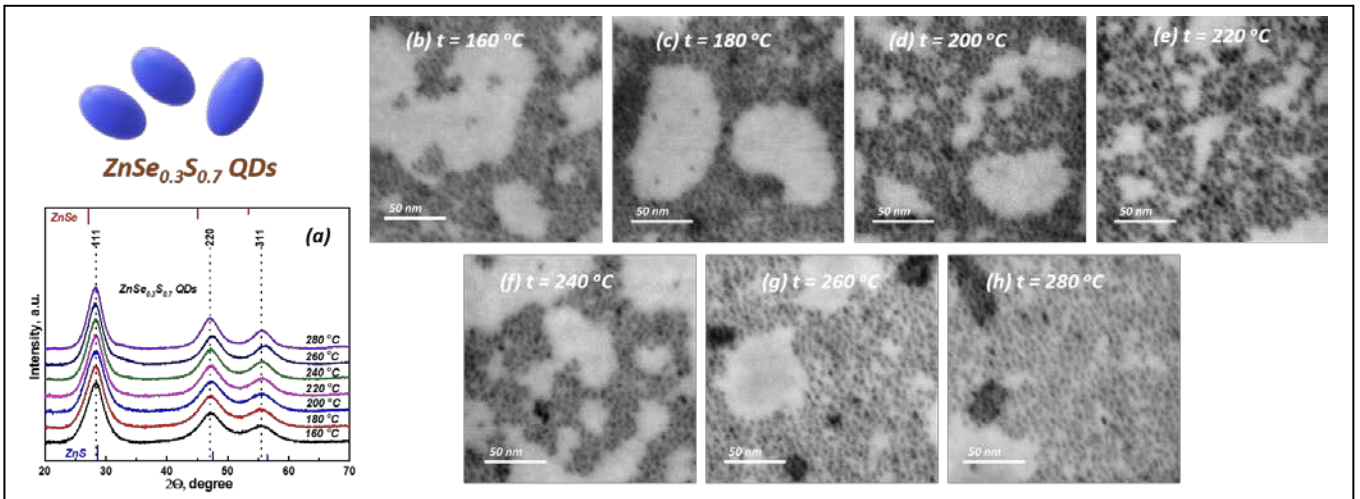

Fig. 3. XRD patterns of $ZnSe_{0.3}S_{0.7}$ QDs (a); STEM images of $ZnSe_{0.3}S_{0.7}$ QDs prepared at 160 °C (b), 180 °C (c), 200 °C (d), 220 °C (e), 240 °C (f), 260 °C (g), 280 °C (h).

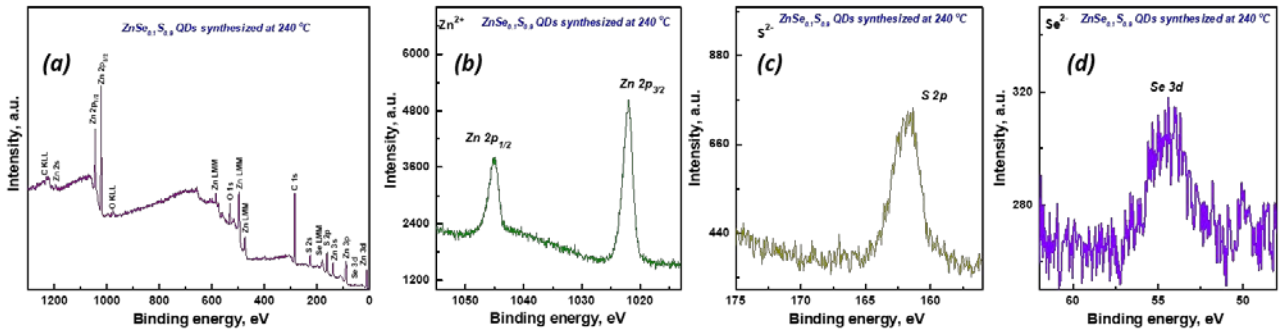

Fig. 4. XPS survey spectra (a), chemical state analysis of Zn *2p* (b), S *2p* (c), and Se *3d* (d) of $ZnSe_{0.1}S_{0.9}$ QDs prepared at 240 °C.

Through the survey spectra, we identified the presence of C, O, Zn, S, and Se in all samples. As an example, the survey spectrum of $ZnSe_{0.1}S_{0.9}$ QDs synthesized at 240 °C is presented (Fig. 4a). Carbon and oxygen peaks correspond to the presence of organic ligands which serve as the QDs protective shell. Fig. 4b displays high resolution (HR) Zn *2p*, where the corresponding spin-orbit Zn $2p_{3/2}$ / Zn $2p_{1/2}$ signals are centered at 1021.9 eV / 1044.9 eV. These binding energies (BEs) suggest the presence of Zn^{2+} [14]. As is depicted in Figure 4c, S *2p* HR spectrum can be deconvoluted into two components corresponding to the spin-orbit splitting S $2p_{3/2}$ / S $2p_{1/2}$ centered at 161.5eV / 162.7eV. Figure 4d demonstrates the HR spectrum of Se *3d*, which can be also deconvoluted into two components where its spin-orbit Se $3d_{5/2}$ / Se $3d_{3/2}$ signals corresponding to Se^{2-} species since they are located at 54.1 eV / 54.9 eV.

B. The optical properties of $ZnSe_{0.1}S_{0.9}$ and $ZnSe_{0.3}S_{0.7}$ QDs

The QDs UV-Vis absorbance (ABS) spectra in the spectral range 200 - 700 nm were measured using UV-3600 (Shimadzu) spectrometer and PL spectra were measured on Fluorometer PTI QuantaMaster 400 (Horiba Scientific) in the spectral range 250 - 850 nm using xenon lamp (75 W) as the excitation source.

During each synthesis, the nucleation and growth of QDs were monitored by taking aliquots from the reaction mixture (20 µl) in 2 ml $CHCl_3$. The temporal evolution of the nucleation and growth ABS spectra of the $ZnSe_{0.1}S_{0.9}$ QDs at 220 °C (Fig. 5a) represents the significant red shift. A similar shift was also observed in the growth of $ZnSe_{0.3}S_{0.7}$ QDs at 200 °C (Fig. 6a), indicating instantaneous nucleation at the moment when the reaction mixture was placed into the Wood's metal bath heated to a given temperature (curves 4 Fig. 5a, b). A further red shift indicates the ongoing growth of nanocrystals. Similar changes in the growth pattern of QDs were also found in the PL spectra (Fig. 5b, 6b), confirming the formation of stable complexes of zinc linoleate with the corresponding thio- and selenoureas. According to curves 1 – 3 in Figures 5b and 6b, these complexes have their own emission spectra. With a sharp increase in temperature to 220 °C (Fig. 5b), the PL intensity increases and the maximum smooths out and shifts to the blue region, which confirms the decomposition of complexes with the release of molecular zinc sulfides and selenides, forming an environment for the nucleation of ZnSeS QDs.

The absorbance and emission spectra of $ZnSe_{0.1}S_{0.9}$ QDs synthesized in the temperature range 160 – 280 °C are presented in Figures 5c-j. With a rise in nucleation and growth temperature of $ZnSe_{0.1}S_{0.9}$ QDs, a red shift of the absorbance edge was detected, which was caused by an increase in the size of QDs (Table 1). In this case, the PL maximum shifts to the blue region and PL QY increases from 9.8 to 24 %. The shift of the PL $ZnSe_{0.1}S_{0.9}$ QDs spectra to the high-energy region, in this case, is associated with the uneven distribution of sulfide and selenide components in the nanocrystal, caused by different rates of entry of

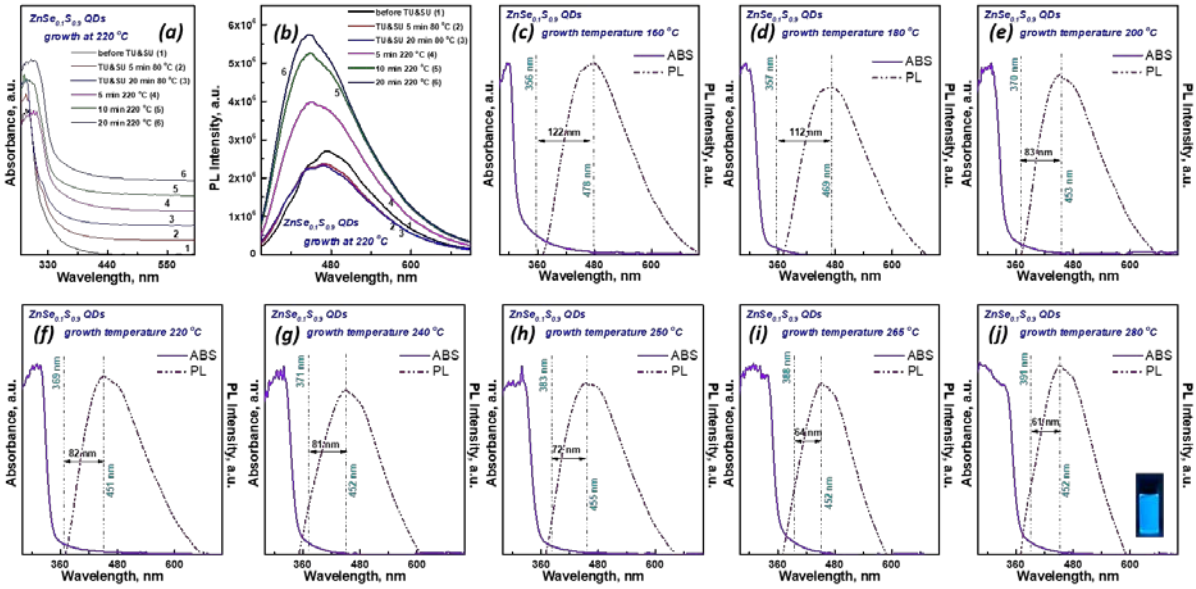

Fig. 5. Temporal evolution of the absorbance (a) and the PL emission spectra (b) of ZnSe0.3S0.7 QDs, prepared at 200 °C; comparison of ABS (solid lines) and PL emission (dashed lines) of ZnSe0.3S0.7 QDs, prepared at 160 °C (c), 180 °C (d), 200 °C (e), 220 °C (f), 240 °C (g), 260 °C (h), 280 °C (i); PL decay kinetic curves of ZnSe0.3S0.7 QDs, prepared at 160 - 280 °C.

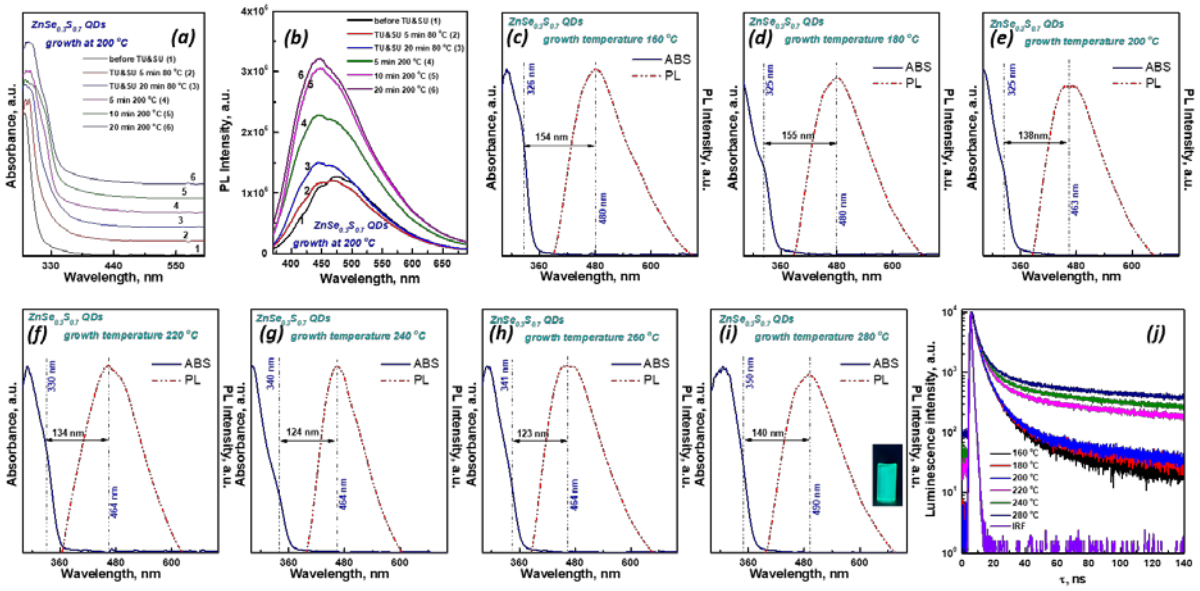

Fig. 6. Temporal evolution of the absorbance (a) and the PL emission spectra (b) of $ZnSe_{0.1}S_{0.9}$ QDs, prepared at 220 ºC; comparison of ABS (solid lines) and PL emission (dashed lines) of $ZnSe_{0.1}S_{0.9}$ QDs, prepared at 160 °C (c), 180 °C (d), 200 °C (e), 220 °C (f), 240 °C (g), 250 °C (h), 265 °C (i), 280 °C (j).

molecular building blocks into the growth medium. The higher reactivity of substituted selenourea provokes a relatively high level of introduction of molecular selenides into the nanocrystal growth medium even at low temperatures. This phenomenon ensures the formation of core/shell-like structured (heterogeneous alloys) $ZnSe_{0.1}S_{0.9}$ QDs with a core enriched in selenides. As the temperature increases, the decomposition of thio-complexes accelerates and the amount of sulfides and selenides in the growth medium becomes equal, which is reflected by a blue shift in the PL spectra, since the band gap of ZnS (3.6 eV) is higher than the band gap of ZnSe (2.58 eV) [15].

With an augmentation in the nucleation temperature, a red shift of the absorption edge and a blue shift of the PL maximum were revealed for $ZnSe_{0.3}S_{0.7}$ QDs synthesized in the temperature range of 160 – 260 °C (Fig. 6c-i). It should be noted that, unlike $ZnSe_{0.1}S_{0.9}$ QDs, the $ZnSe_{0.3}S_{0.7}$ QDs sizes almost did not change (Table 1). At the nucleation temperature of 200 °C, the rates of decomposition of thio- and seleno-complexes were equalized. It causes a significant blue shift of the PL spectra, which retains its position until the nucleation temperature of 260 °C is reached. A further increase in temperature to 280 °C leads to a red shift of the PL maximum (from 464 nm to 490 nm), which was probably caused by the relatively high release of selenide into the nanocrystal growth medium.

A similar phenomenon was also observed in the quenching kinetics of $ZnSe_{0.3}S_{0.7}$ QDs, which were nucleated at different temperatures (Fig. 6j). The PL lifetime measurements were performed using TCSPC accessories for Fluorometer PTI QuantaMaster 400 with 361 nm light pulse excitation and the pulse half-width 0.8 ns produced by NanoLED 360 (Horiba Scientific). PL decay kinetics curves were analyzed by PTI Felix GX software. $ZnSe_{0.3}S_{0.7}$ QDs synthesized at 160 – 200 °C demonstrated fast quenching kinetics ($\tau_{avg} \approx 1.6$ ns). An increase in the nucleation temperature to 220 ° C brings a sharp jump in τ_{avg} up to 4.13 ns due to a change in the intensity of the long component (Fig. 6j), which is associated with an increase in the number of surface-traps defects.

TABLE I. AVERAGE CRYSTALLINE SIZE, CHALCOGEN RATIO AND OPTICAL PROPERTIES OF $ZnSe_{0.1}S_{0.9}$ AND $ZnSe_{0.3}S_{0.7}$. PEAK MAXIMUM IN THE ABS SPECTRA (Λ_{ABS}), EXCITATION WAVELENGTH (Λ_{EXC}), PEAK MAXIMUM IN THE PL SPECTRA (Λ_{EM}), STOKES SHIFT, PL QY AND AVERAGE PL LIFETIME (τ_{AVG}).

Composition / Temperature / Se : S Ratio	Size, nm	Optical parameters					
		λ_{ABS}, nm	λ_{exc}, nm	λ_{em}, nm	Stokes shift, nm	PL QY, %	τ_{avg}, ns
$ZnSe_{0.1}S_{0.9}$ / 160 °C / 9.9 : 90.1	2.52	356	360	478	122	9.8	-
$ZnSe_{0.1}S_{0.9}$ / 180 °C / 8.8 : 91.2	2.80	357	360	469	112	10.1	-
$ZnSe_{0.1}S_{0.9}$ / 200 °C / 9.0 : 91.0	3.35	370	360	453	83	9.9	-
$ZnSe_{0.1}S_{0.9}$ / 220 °C / 9.2 : 90.8	4.04	369	360	451	82	15.6	-
$ZnSe_{0.1}S_{0.9}$ / 240 °C / 10.2 : 89.8	4.05	371	342	452	81	19.6	-
$ZnSe_{0.1}S_{0.9}$ / 250 °C / 10.1 : 89.9	4.10	383	360	455	72	24.0	-
$ZnSe_{0.1}S_{0.9}$ / 265 °C / 10.0 : 90.0	4.15	388	360	452	64	18.4	-
$ZnSe_{0.1}S_{0.9}$ / 280 °C / 9.5 : 90.5	4.15	391	360	452	61	18.2	-
$ZnSe_{0.3}S_{0.7}$ / 160 °C / 29.3 : 70.7	2.87	326	380	480	154	10.1	1.69
$ZnSe_{0.3}S_{0.7}$ / 180 °C / 31.0 : 69.0	3.05	325	376	480	155	11.9	1.62
$ZnSe_{0.3}S_{0.7}$ / 200 °C / 28.5 : 71.5	3.37	325	375	463	138	10.4	1.67
$ZnSe_{0.3}S_{0.7}$ / 220 °C / 28.4 : 71.6	3.73	330	365	464	134	9.8	4.13
$ZnSe_{0.3}S_{0.7}$ / 240 °C / 27.9 : 72.1	3.67	340	362	464	124	15.8	5.95
$ZnSe_{0.3}S_{0.7}$ / 260 °C / 27.6 : 72.4	3.52	341	364	464	123	16.1	-

$ZnSe_{0.3}S_{0.7}$ / 280 °C / 27.2 : 72.8	3.55	350	375	490	140	15.2	8.32

Energy dispersion X-Ray microanalysis of all synthesized QDs (EDS) was carried out using scanning electron microscope LYRA 3 (Tescan, Czech Republic) equipped with EDS analyzer Aztec X-Max 20 (Oxford Instruments) at acceleration voltage 20 kV. The elemental analysis data (Zn, Se, S) of the synthesized QDs are close to the nominal composition. In addition, carbon and traces of oxygen and nitrogen were found in the EDS spectra, corresponding to zinc linoleate and OAm that build up the protective shell of QDs.

IV. Conclusions

In this study, a new approach to the synthesis of ZnSeS QDs was presented, combining one-pot and hot-injection methods with the formation of stable intermediate complexes of zinc linoleate with substituted thio- and selenoureas. The thio- and seleno-complexes coexisting in the QDs nucleation and growth medium decompose into molecular sulfides and selenides at different rates, which can be influenced by operating the N-substituents. This phenomenon ensures the formation of crystals with different distribution of elements from homogeneous to core/shell-like structured alloys. Temperature-resistant crystal structure, uniformity in shape and size, and bright PL feature the $ZnSe_{0.}1S_{0.9}$ and $ZnSe_{0.3}S_{0.7}$ QDs synthesized by this method, thereby opening pathways for an extension to other compositions of multicomponent chalcogenides.

Acknowledgment

The authors appreciate the financial support from the project “High-sensitive and low-density materials based on polymeric nanocomposites” - NANOMAT (No. CZ.02.1.01/0.0/0.0/17_048/0007376) and grant LM2018103 from the Ministry of Education, Youth and Sports of the Czech Republic.

References

[1] A. A. P. Mansur, H. S. Mansur, R. L. Mansur, F. G. de Carvalho, and S. M. Carvalho, “Bioengineered II–VI semiconductor quantum dot-carboxymethylcellulose nanoconjugates as multifunctional fluorescent nanoprobes for bioimaging live cells,” Spectrochimica Acta Part A: Molecular and Biomolecular Spectroscopy, Vol. 189 pp. 393–404, January 2018.

[2] D.-W. Shin, Y.-H. Suh, S. Lee, B. Hou, S. D. Han, Y. Cho, X.-B. Fan, S. Y. Bang, S. Zhan, J. Yang, H. W. Choi, S. Jung, F. C. Mocanu, H. Lee, L. Occhipinti, Y. T. Chun, G. Amaratunga, and J. M. Kim, “Waterproof flexible InP@ZnSeS quantum dot light-emitting diode,” Adv. Optical Mater., Vol. 8, p. 1901362, April 2020.

[3] X. Li, Q. Lin, J. Song, H. Shen, H. Zhang, L. S. Li, X. Li, and Z. Du, “Quantum-dot light-emitting diodes for outdoor displays with high stability at high brightness,” Adv. Optical Mater., Vol. 8, p. 1901145, January 2020.

[4] H. Kang, S. Kim, J. H. Oh, H. C. Yoon, J.-H. Jo, H. Yang, and Y. R. Do, “Color-by-blue QD-emissive LCD enabled by replacing RGB color filters with narrow-band GR InP/ZnSeS/ZnS QD films,” Adv. Optical Mater., Vol. 6, p. 1701239, June 2018.

[5] M. M. Islam, S. Ishizuka, A. Yamada, K. Sakurai, S. Niki, T. Sakurai, and K. Akimoto, “CIGS solar cell with MBE-grown ZnS buffer layer,” Solar Energy Materials & Solar Cells, Vol. 93, pp. 970–972, June 2009.

[6] H. X. Chuo, T. Y. Wang, and W. G. Zhang, “Optical properties of ZnS_xSe_{1-x} alloy nanostructures and their photodetectors,” Journal of Alloys and Compounds, Vol. 606, pp. 231–235, April 2014.

[7] J. M. Park, H. J. Kim, Y. S. Hwang, D. H. Kim, and H. W. Park, “Scintillation properties of quantum-dot doped styrene based plastic scintillators,” Journal of Luminescence, Vol. 146, pp. 157–161, February 2014.

[8] C. Liu, Z. Li, T. J. Hajagos, D. Kishpaugh, D. Y. Chen, and Q. Pei, “Transparent ultra-high-loading quantum dot/polymer nanocomposite monolith for gamma scintillation,” ACS Nano, Vol. 11, Issue 6, pp. 6422–6430, May 2017.

[9] C. L. Wang, L. Gou, J. M. Zaleski, and D. L. Friesel, “ZnS quantum dot based nanocomposite scintillators for thermal neutron detection,” Nuclear Instruments and Methods in Physics Research A, Vol. 622, Issue 1, pp. 186-190, October 2010.

[10] M.-R. Gao, Y.-F. Xu, J. Jiang, and S.-H. Yu, “Nanostructured metal chalcogenides: synthesis, modification, and applications in energy conversion and storage devices,” Chem. Soc. Rev., Vol. 42, pp. 2986-3017, January 2013.

[11] L. S. Hamachi, I. Jen-La Plante, A. C. Coryell, J. De Roo, and J. S. Owen, “Kinetic control over CdS nanocrystal nucleation using a library of thiocarbonates, thiocarbamates, and thioureas,” Chem. Mater., Vol. 29, pp. 8711–8719, October 2017.

[12] A. Iakovleva, L. Loghina, Z. Olmrova Zmrhalova, J. Mistrik, P. Svec, S. Slang, K. Palka, and M. Vlcek, “Environmentally friendly approach to the synthesis of monodisperse and bright blue emitting $Cd_{0.15}Zn_{0.85}S$ quantum dots,” Journal of Alloys and Compounds, Vol. 812, p. 152159, January 2020

[13] M. Chylii, L. Loghina, A. Kaderavkova, S. Slang, P. Svec, J. Rodriguez Pereira, B. Frumarova, D. Cizkova, A. Bezrouk, and M. Vlcek, “Enhanced optical properties of $ZnSe_xS_{1-x}$ and Mn-doped $ZnSe_xS_{1-x}$ QDs via non-toxic synthetic approach,” Materials Chemistry and Physics, Vol. 284, p. 126060, May 2022.

[14] J. Zimdars, J. Pilger, M. Entrup, D. Deiting, A. H. Schafer, and M. Bredol, A facile synthesis of alloyed Mn-doped ZnSeS nanoparticles using a modified selenium/sulfur precursor in a one-pot approach,” : New J. Chem., Vol. 40, p. 8465, August 2016.

[15] M. A. Aviles, J. M. Cordoba, M. J. Sayagues, and F. J. Gotor, “Tailoring the band gap in the ZnS/ZnSe system: solid solutions by a mechanically induced self-sustaining reaction,” Inorg. Chem., Vol. 58, pp. 2565–2575, January 2019.

Ministry of Education, Youth and Sports of the Czech Republic.